Materials & Design 263 (2026) 115584

Contents lists available at ScienceDirect

Materials & Design

journal homepage: www.elsevier.com/locate/matdes

Modular metamaterials with deep learning–enabled customizable stress–strain responses

Xiaofeng Guo[a], Miaomiao He[b], Ikumu Watanabe[c], Jiaxin Zhou[c], Takayuki Yamada[d], Yong Yi[a,*], Xiaoyang Zheng[d,*]

[a] School of Materials Science and Engineering, Southwest University of Science and Technology, Mianyang 621010, China
[b] College of Biomedical Engineering, School of Chemical Engineering, Sichuan University, Chengdu 610065, China
[c] Center for Basic Research on Materials, National Institute for Materials Science, 1-2-1 Sengen, Tsukuba 305-0047, Japan
[d] Institute of Engineering Innovation, Graduate School of Engineering, The University of Tokyo, Tokyo 113-8656, Japan

HIGHLIGHTS

- A novel class of modular metamaterials with customizable stress–strain curves was proposed.
- Deep learning models accelerate the property prediction and inverse design of the modular metamaterials.
- Inversely designed sample was validated using experiment and simulation.

GRAPHICAL ABSTRACT

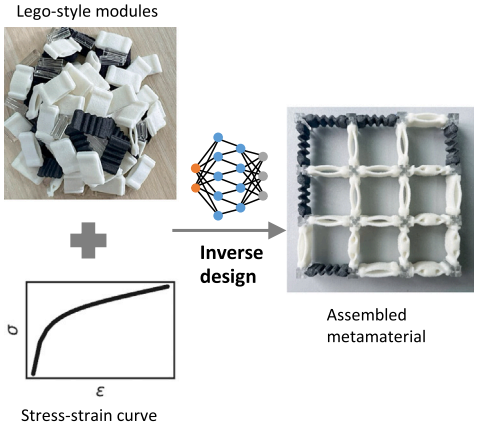

ARTICLE INFO

Keywords:
Mechanical metamaterial
Deep learning
Inverse design
Nonlinear mechanical property
Modular material

ABSTRACT

Modular mechanical metamaterials offer unique opportunities for programmable and reconfigurable functionality through simple geometric rearrangements. Inspired by the modularity of Lego blocks, we propose a new class of modular metamaterials composed of three standardized modules—linear, yielding-like, and snap-through buckling elements—that can be assembled into two- and three-dimensional grids to realize diverse nonlinear stress–strain responses. To accelerate design and optimization, we integrate deep learning (DL) with the metamaterial design process. A convolutional neural network-based predictor rapidly estimates the stress–strain curves of given modular configurations, achieving a prediction accuracy of $R^2 > 0.999$. Furthermore, a conditional variational autoencoder-based inverse designer enables the automatic generation of modular configurations that match target stress–strain curves, demonstrating high fidelity ($R^2 \approx 0.97$). The proposed DL framework allows rapid, scalable, and reprogrammable design of nonlinear mechanical responses without exhaustive simulations or manual tuning. This study establishes a universal, data-driven strategy for the inverse design of modular metamaterials, paving the way toward intelligent, reconfigurable material systems for applications in soft robotics and adaptive structures.

* Corresponding authors.
Email addresses: yiyong@swust.edu.cn (Y. Yi), xyzheng1995@gmail.com (X. Zheng).

https://doi.org/10.1016/j.matdes.2026.115584
Received 22 November 2025; Received in revised form 14 January 2026; Accepted 29 January 2026
Available online 30 January 2026

1. Introduction

Mechanical metamaterials, composed of periodically arranged building blocks, are artificially engineered materials whose exceptional properties and functions arise from their microstructures and constituent materials [1–5]. By precisely tailoring the type, connectivity, and spatial arrangement of their structural elements, metamaterials can exhibit performance far surpassing that of their base materials. Notable examples include ultralight and ultrastiff lattices [6,7], auxetic metamaterials with negative Poisson's ratios [8–10], multistable metamaterials with reconfigurable shapes [11,12], origami- and kirigami-inspired architectures with deployable geometries [13,14], and stimuli-responsive metamaterials capable of in situ adaptation to external environments [2,15,16]. These unique properties and functionalities have enabled the deployment of metamaterials in a wide range of applications, including robotics [17,18], impact-absorbing and wearable devices [19,20], actuators [21], tissue engineering [22,23], and mechanical computing [24,25].

Particularly, nonlinear mechanical responses have attracted significant attention, as controlling such responses under large deformations can unlock advanced functionalities in emerging fields such as force transmission and soft robotics [17]. For instance, metamaterials with tailored stress–strain behaviors can emulate the nonlinear actuation mechanisms found in natural systems such as the Venus flytrap and mantis shrimp, enabling rapid motion and energy release through snap-through instabilities [26,27]. In mechanical metamaterials, these nonlinear responses often arise from complex physical mechanisms including mechanical instabilities (e.g., buckling) and frictional self-contact [28,29]. Although computational approaches such as the finite element method (FEM) can be employed to explore the design and property spaces of metamaterials, their high computational cost poses a major bottleneck for automatic material discovery targeting desired properties or nonlinear behaviors—a process commonly referred to as inverse design [30].

Recent advancements in deep learning (DL) have revolutionized the design and discovery of mechanical metamaterials [1,31]. For instance, the effective properties of metamaterials can be accurately predicted using multilayer perceptrons (MLPs) [32,33] and convolutional neural networks (CNNs) [34]. Conditional deep generative models—such as generative adversarial networks (GANs) [35,36], variational autoencoders (VAEs) [37], and diffusion models [38,39]—enable the inverse design of metamaterials with target properties. Such data-driven inverse design frameworks can significantly reduce reliance on human intuition and experience, eliminating the need for inefficient trial-and-error procedures. Recent studies have demonstrated the potential of AI-driven approaches for the inverse design of metamaterials with nonlinear mechanical responses, including conditional diffusion models [38] and autoregressive graph-based frameworks [40]. However, the metamaterials generated by these approaches are typically bulky microstructures, which limit their manufacturability and reconfigurability compared with modular architectures. Modular metamaterials—composed of repeating, interchangeable building blocks or structural elements—can be mass-produced using conventional or additive manufacturing techniques and subsequently assembled and reconfigured into diverse architectures. The modularity of mechanical metamaterials significantly enhances manufacturability by standardizing building blocks and decoupling geometric complexity from fabrication.

The concept of modularity has been explored in reconfigurable metamaterials based on discrete elements such as lattices and multistable unit cells. Traditionally, modular metamaterials are composed of periodic, unified unit cells [41,42], which can be employed to demonstrate robust, collective, and automated assembly and reconfiguration of large-scale structures [43]. Further, motorized unit cells have been incorporated into modular swarm robotic systems to enable autonomous locomotion and extreme shape-morphing versatility [44]. This modularity is particularly advantageous in unstructured environments for adaptable robotics. Expanding the diversity of module types further allows the design of multimodal, multistable, and reprogrammable machines [45], and large-scale design databases have been leveraged to automatically mine extreme mechanical properties [46]. In this work, in contrast to these prior approaches, we standardize metamaterial modules and explicitly decouple the nonlinear responses of individual unit cells, thereby simplifying fabrication and enabling more efficient and scalable automated assembly. The three standardized modules with decoupled nonlinear responses enable a broader design space compared to their unified, homogeneous counterparts.

Inspired by the modularity of Lego blocks, we propose a new class of modular metamaterials composed of three types of structural modules, whose design is accelerated by DL (Fig. 1). The configurations of these modular metamaterials with customizable nonlinear stress–strain responses can be automatically generated through a deep-learning-based inverse design framework. Specifically, we designed two-dimensional (2D) and three-dimensional (3D) structural modules exhibiting three characteristic stress–strain behaviors—linear, yielding-like (with a plateau region in the stress–strain curve formed by ligament bending), and snap-through buckling—to establish a broad design space. We then constructed 2D and 3D labeled datasets of modular metamaterials with various configurations using FEM simulations. Based on the datasets, CNN-based predictors were trained to predict stress–strain curves, and conditional VAE-based inverse designers were developed to generate modular configurations that achieve target stress–strain responses.

2. Results and discussion

2.1. Lego-inspired modules

The proposed modular metamaterials are inspired by Lego bricks, where each brick serves as a standardized, reusable module that can be connected in countless configurations through simple geometric rules (studs and holes). The same set of bricks can construct a car, a castle,

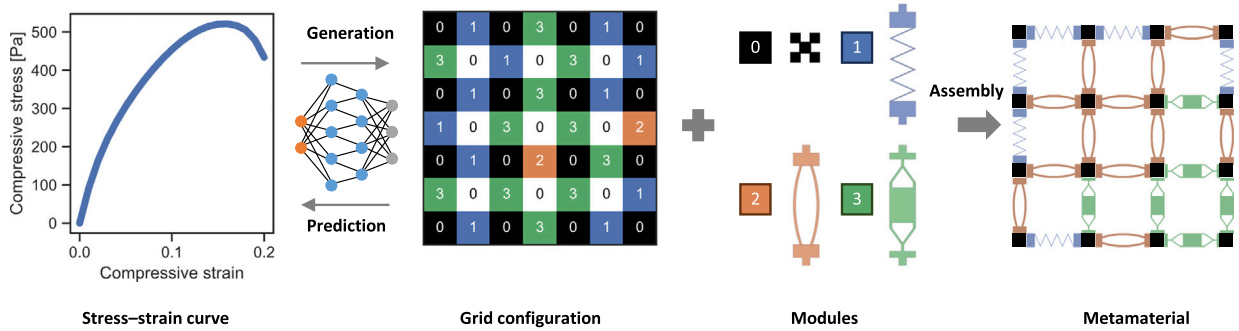

Fig. 1. Overview of the proposed framework. Modular metamaterials, reconfigurable through standardized building modules, exhibit diverse nonlinear stress–strain responses. Deep learning models are utilized for rapid stress–strain curve prediction and inverse design of modular configurations. The resulting metamaterials are physically assembled from 3D-printed modules according to the generated grid configurations.

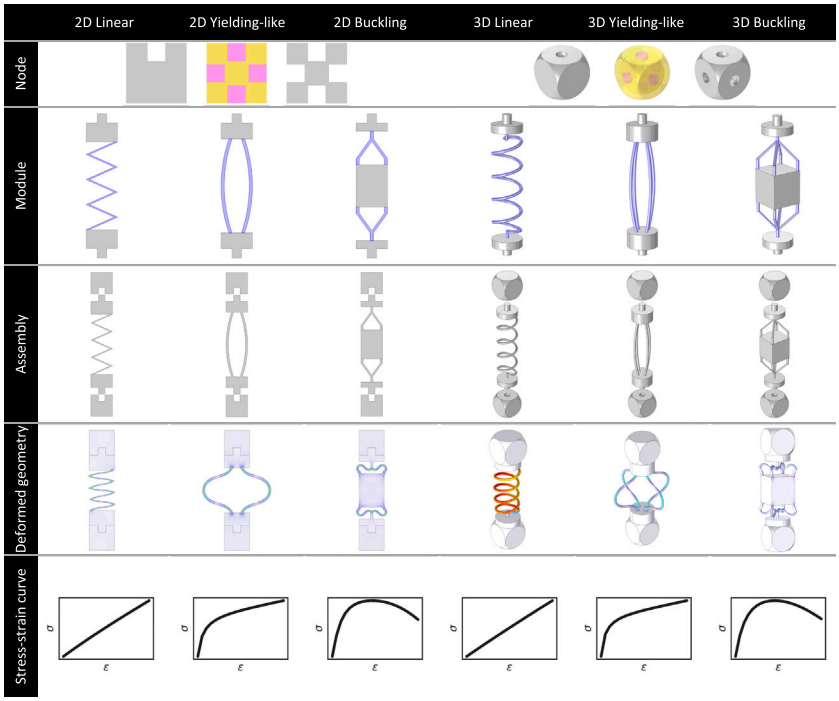

Fig. 2. Designs of 2D and 3D modules for modular metamaterials. Each module exhibits a distinctive mechanical response—linear, yielding-like, or snap-through buckling—and the modules can be assembled via node joints.

or a robot—merely by rearranging them. Following this concept, we designed three standardized modules for both 2D and 3D metamaterials. Each 2D or 3D module exhibits a distinctive mechanical response, including linear, yielding-like, and snap-through buckling behaviors (Fig. 2 and Fig. S1). These modules are assembled into 2D or 3D grids via node joints, where the protruding tenons at the ends of the modules fit snugly into the mortises of the joints. The resulting modular metamaterials inherit Lego's geometric reconfigurability, enabling customizable and reprogrammable macroscopic behaviors through the rearrangement of the microstructural modules. To ensure that the stress–strain curves of the three modules remain within comparable magnitudes, we employed different 3D-printable materials: a hard rubber-like material (incompressible neo-Hookean hyperelastic model, $E = 85$ MPa) for the linear module; a soft rubber-like material (incompressible neo-Hookean hyperelastic model, $E = 3.35$ MPa) for the yielding-like and snap-through buckling modules; and a rigid resin (elastic model, $E = 1.6$ GPa, $\nu = 0.23$) for the node joints.

The linear module, characterized by a spring-like geometry, deforms primarily through elastic compression of its elements, resulting in a linear stress–strain response. The yielding-like module, composed of slender ligaments, deforms mainly via ligament bending and exhibits a stress–strain curve with an initial linear region followed by a plateau. The snap-through buckling module, consisting of a three-bar structure, deforms through snap-through instabilities of the bars, producing a stress–strain curve with a linear region followed by a sudden jump. Furthermore, the stiffness of each module can be tuned by adjusting its thickness, thereby expanding the design space of the modular metamaterial system (Figs. S2–S4). For the 2D dataset prepared with a fixed module thickness of 2 mm, the design space can be extended to a much larger set of stress–strain responses by introducing multiple thickness levels (e.g., 1, 2, and 3 mm). For instance, modular metamaterials exhibiting multi-stage stress–strain behavior can be realized by combining buckling modules with different thicknesses. However, because each metamaterial is represented by a 7×7 grid containing 24 ligament modules and 16 node modules, the number of possible configurations increases exponentially—from 3^{24} to 9^{24}—which dramatically raises the computational cost of both dataset generation and deep learning model training. The deep learning framework proposed in this work can also be easily applied to the extended dataset by tuning the input and output layers of neural networks and retraining them using the new dataset.

2.2. Stress–strain curve prediction

To accelerate the discovery of modular metamaterials, we developed a CNN-based predictor for the stress–strain curve prediction of 2D modular systems. The CNN was trained on a labeled dataset comprising 60,000 modular metamaterials with distinct configurations and their corresponding stress–strain curves, which were obtained through FEM simulations. Each metamaterial configuration was represented as a 7×7 grid containing 24 ligament modules and 16 node modules (Fig. 1), where the grid values denote different module types (Fig. 3(b)). The 2D CNN-based predictor consists of three convolutional blocks—each including convolutional, batch normalization, and dropout layers—followed by global average pooling and an MLP composed of three dense layers (Fig. 3(a)). The model takes a batch of 7×7 grid representations as input and outputs predicted stress–strain curves in the form of a 1D sequence of 21 stress values corresponding to uniformly sampled strain levels up to $\varepsilon = 0.2$. After training, the predictor achieved ultrahigh accuracy with $R^2 > 0.999$, as illustrated in Fig. 3(c), where 16 randomly selected metamaterial configurations were evaluated. These results confirm that the proposed CNN predictor can rapidly and accurately estimate the stress–strain behavior of modular metamaterials—at a computational cost of less than one second per sample—significantly faster than conventional FEM simulations. Moreover, the framework can be readily extended to metamaterials with arbitrary grid sizes and configurations.

To further demonstrate the robustness and generality of the CNN-based predictor, we developed a 3D predictor based on a 3D CNN to predict the stress–strain curves of 3D modular metamaterials. A labeled 3D dataset was constructed, in which each modular metamaterial was

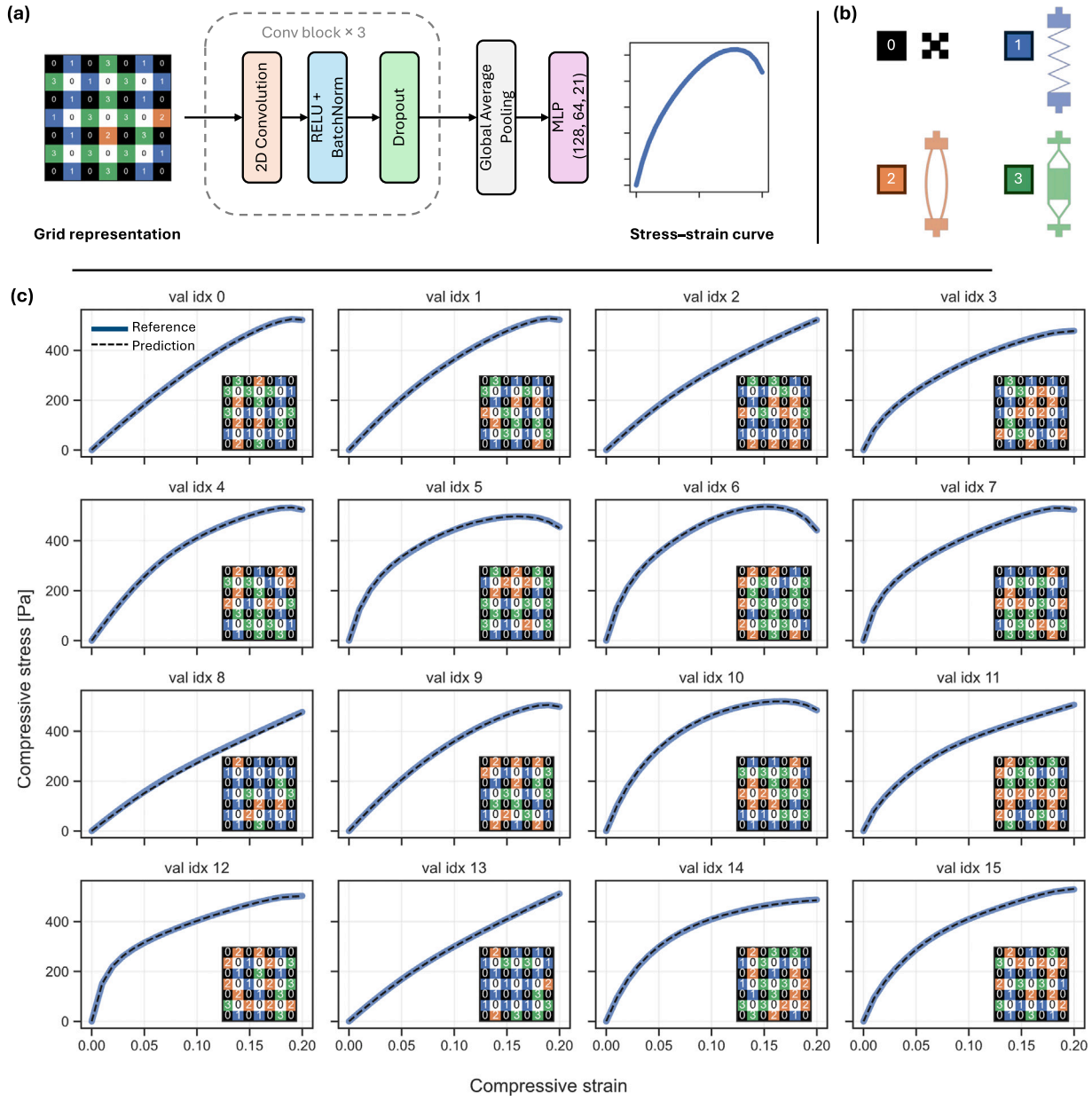

Fig. 3. Prediction of stress–strain curves for 2D modular metamaterials using a CNN-based predictor. (a) Architecture of the 2D CNN predictor. (b) 2D modular representations. (c) Representative predicted stress–strain curves obtained from the trained 2D predictor.

generated by randomly assembling 3D modules into a $5 \times 5 \times 5$ grid and subsequently analyzed using FEM simulations to obtain its stress–strain curve. The dataset consisted of 60,000 samples, each represented by a $5 \times 5 \times 5$ grid containing 54 ligament modules and 27 node modules (Fig. S5). The 3D CNN-based predictor adopts a similar architecture to its 2D counterpart, with the convolutional and global average pooling layers replaced by their 3D analogues (Fig. 4(a)). It takes a batch of $5 \times 5 \times 5$ grid representations as input and outputs predicted stress–strain curves in the form of 1D sequences. Trained on the 3D dataset, the predictor achieved ultrahigh prediction accuracy with $R^2 > 0.999$, as illustrated in Fig. 4(c), where 16 randomly selected metamaterial configurations were evaluated. These results confirm that the 3D predictor can accurately and efficiently evaluate the stress–strain responses of modular metamaterials, demonstrating that the CNN-based framework is universally applicable to modular metamaterials represented by grid architectures.

2.3. Inverse design

Inverse design of modular metamaterials enables the automatic discovery of optimal module arrangements to achieve target mechanical properties or behaviors. Instead of relying on trial-and-error assembly, DL-based inverse design establishes a mapping from desired macroscopic responses to the discrete combinations of modules that produce them—allowing rapid, scalable, and reprogrammable material design. Here, we demonstrate the feasibility of DL for the inverse design of modular metamaterials by proposing an inverse designer based on a conditional VAE (Fig. 5(a)). The conditional VAE consists of an encoder and a decoder. The encoder compresses metamaterial grids and their corresponding stress–strain curves into a latent space, and the decoder reconstructs or generates metamaterial grids conditioned on both the latent variables and the target stress–strain curves. During inference, the target stress–strain curve is embedded using an MLP and concatenated

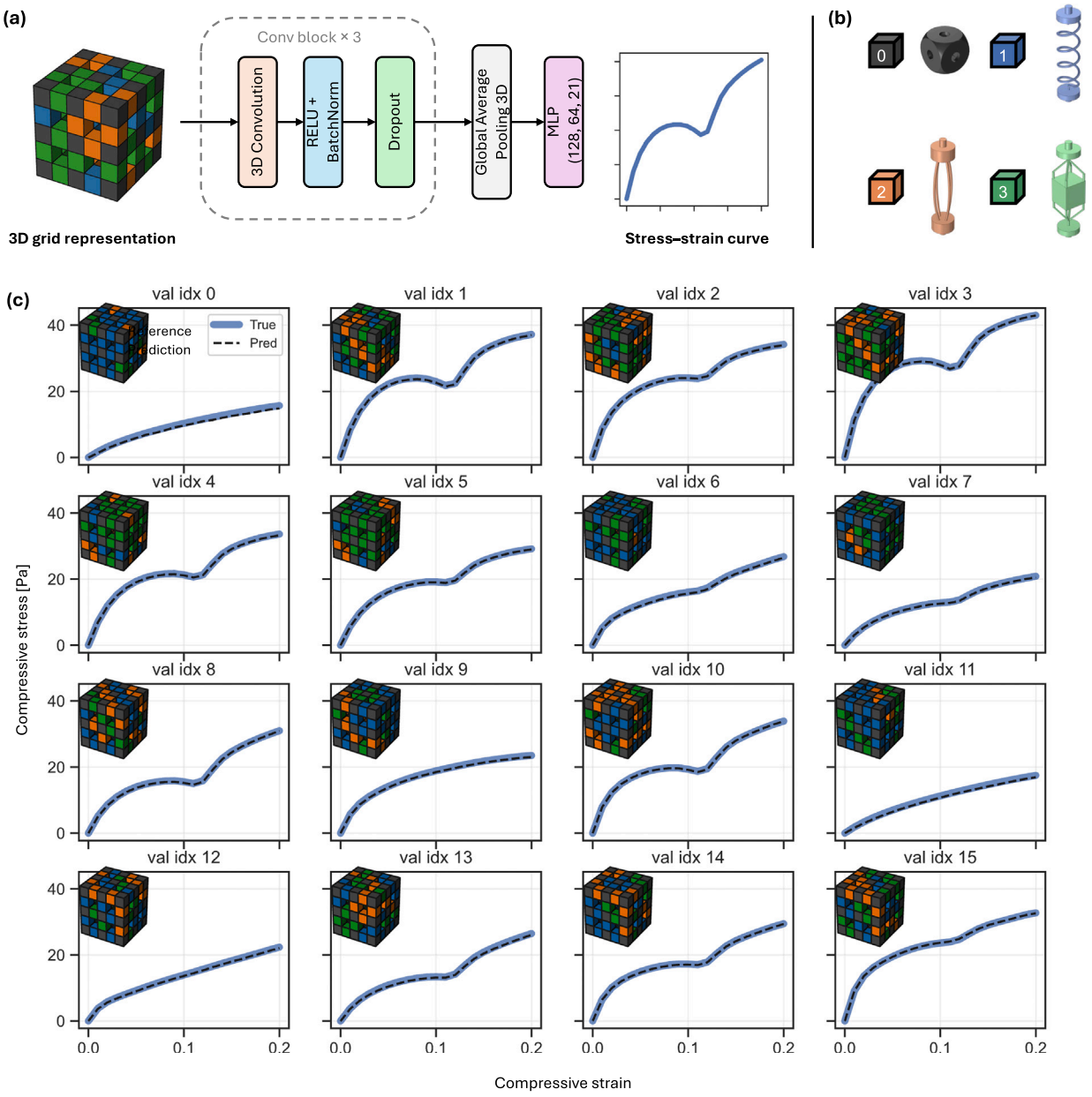

Fig. 4. Prediction of stress–strain curves for 3D modular metamaterials using a 3D CNN-based predictor. (a) Architecture of the 3D CNN predictor. (b) 3D modular representations. (c) Representative predicted stress–strain curves obtained from the trained 3D predictor.

with a randomly sampled latent vector, which is then passed to the decoder to generate candidate metamaterial grids. A pretrained CNN-based predictor is appended after the conditional VAE to evaluate the stress–strain curves of the generated metamaterials. This setup enables a generate-and-rank strategy, where multiple candidates are generated by the conditional VAE and the top-scoring samples are selected as optimal designs according to the R^2 values of their stress–strain curves.

The inverse designer was trained using the aforementioned 2D labeled dataset. For each inference, 16 candidate designs were generated for a given target stress–strain curve, and the four top-scoring samples were selected based on their R^2 values (Fig. 5(b),(c)). Fig. 5(b) compares three target stress–strain curves with those of the generated metamaterials, showing excellent agreement ($R^2 \approx 0.98$). Although slightly lower than the accuracy of the forward predictor, the high R^2 value demonstrates that the inverse designer can successfully generate modular metamaterials whose stress–strain responses closely match the specified targets.

We further extended the inverse designer to 3D modular metamaterials by replacing the convolutional layers in the conditional VAE with their 3D counterparts (Fig. 6(a)). The 3D inverse designer was trained using the 3D labeled dataset and evaluated with the pretrained 3D predictor. For reference, four top-scoring samples were generated for three representative target stress–strain curves (Fig. 6(b),(c)). Similar to the 2D case, the generated 3D modular metamaterials reproduced the target stress–strain curves with high fidelity ($R^2 \approx 0.97$), confirming that the proposed conditional VAE-based framework is robust and generalizable for the inverse design of modular metamaterials with arbitrary grid architectures.

2.4. Experiment validation

To demonstrate the capability of the inverse designer for practical prototyping, we generated a top-scoring 2D metamaterial corresponding to a target stress–strain curve using the trained 2D inverse designer.

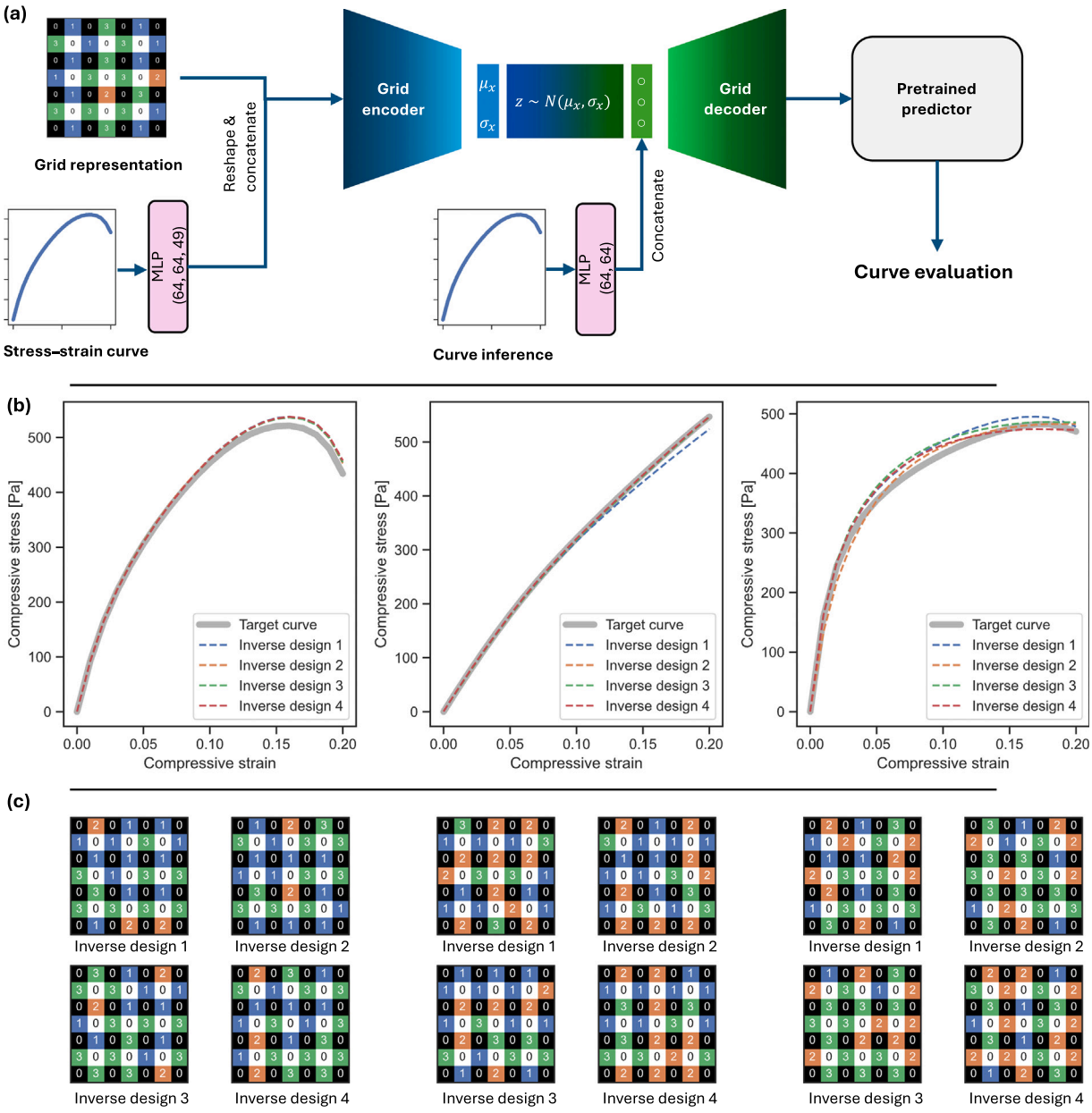

Fig. 5. Inverse design of 2D modular metamaterials with target stress–strain curves using a conditional VAE-based inverse designer. (a) Architecture of the 2D conditional VAE inverse designer. (b) Comparison between the target stress–strain curves and those of the generated metamaterials. (c) Grid representations of the inverse-designed metamaterials.

Based on the resulting grid configuration, we then assembled a modular metamaterial using 3D-printed Lego-style modules (Fig. 7(a),(b)). The modular metamaterial was manually assembled into a 7×7 grid, where the protruding tenons on the ends of the ligament modules interlock with the mortises of the node joints. The mechanical response of the assembled metamaterial was subsequently investigated through uniaxial compression testing. Fig. 7(c) shows the sequence of progressive deformation configurations obtained experimentally, together with FEM simulations. The results exhibit good agreement in deformation patterns between experiment and simulation, confirming the robustness of the FEM model. The stress–strain curves from experiment and simulation are also compared with the target curve (Fig. 7(a)), showing close correspondence. Given the agreement between experiment and simulation, we further performed more validations for different curves (e.g., monotonic hardening, negative stiffness, and multi-stage plateau) through FEM simulations, as shown in Figure S10. These results demonstrate that the framework can robustly generate modular configurations matching diverse nonlinear target responses. Overall, these results validate the reliability of the inverse designer in achieving modular metamaterials with target mechanical behaviors, highlighting its potential for practical applications such as soft robotic components.

3. Conclusion

In conclusion, we propose a new class of modular metamaterials inspired by Lego blocks. The versatility of the designed modules enables the assembly of metamaterials with targeted nonlinear mechanical responses. Their intrinsic reconfigurability allows customizable and reprogrammable macroscopic behaviors to be achieved simply by rearranging microstructural modules. Moreover, the 3D-printable modules can be assembled into complex 3D configurations, offering a

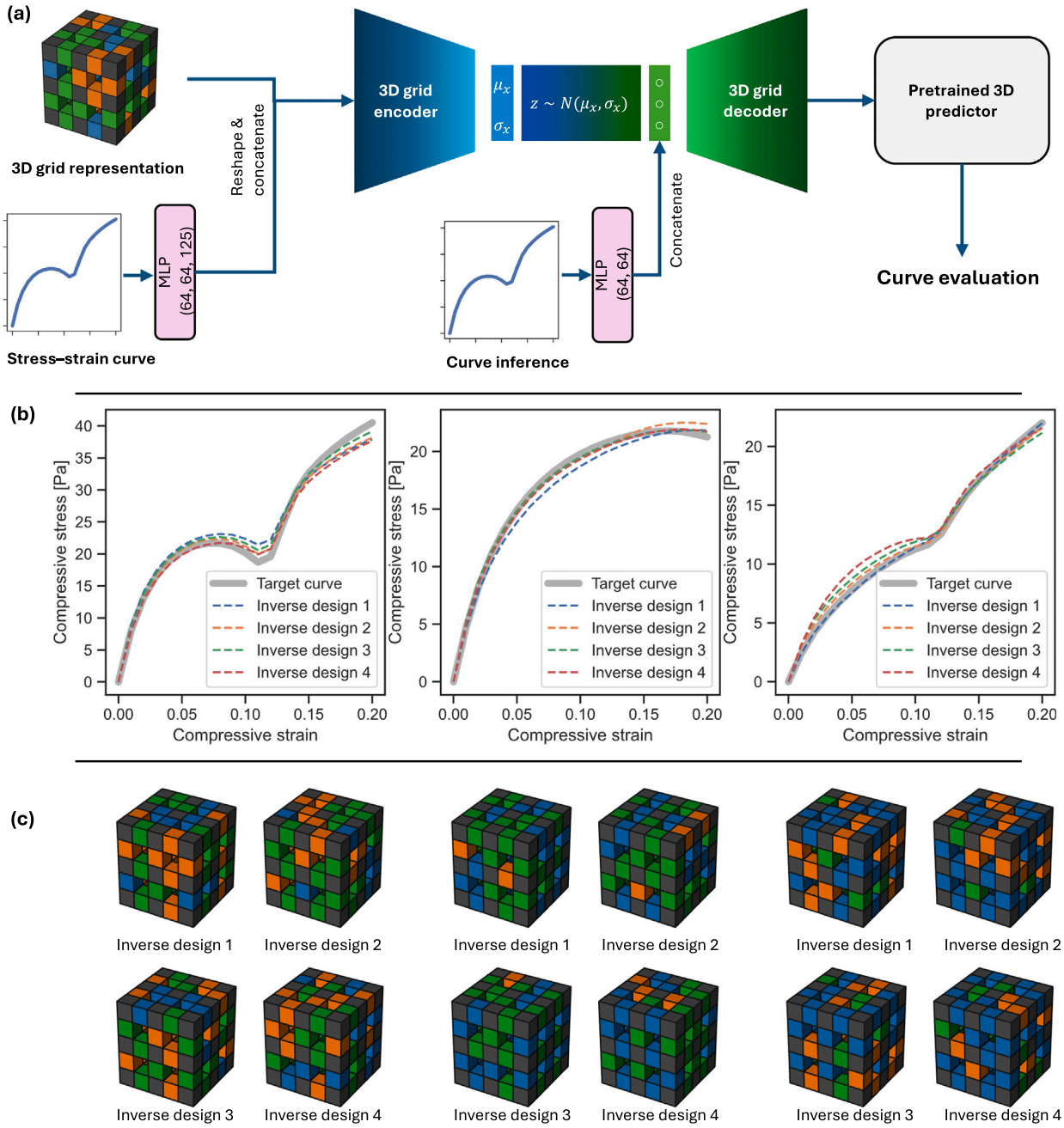

Fig. 6. Inverse design of 3D modular metamaterials with target stress–strain curves using a 3D conditional VAE-based inverse designer. (a) Architecture of the 3D conditional VAE inverse designer. (b) Comparison between the target stress–strain curves and those of the generated metamaterials. (c) 3D Grid representations of the inverse-designed metamaterials.

simpler and more robust fabrication route compared to conventional monolithic 3D-printed metamaterials. The design process is accelerated by DL, where a CNN-based predictor and a conditional VAE-based inverse designer are employed for property prediction and inverse design, respectively. These models enable the rapid generation of optimal modular metamaterials with customizable stress–strain responses through a generate-and-rank strategy, with a high fidelity of $R^2 \approx 0.98$ for 2D inverse design and $R^2 \approx 0.97$ for 3D inverse design. The framework can further evolve into a more interactive and physically consistent design paradigm by integrating large language models [47] and physics-informed machine learning [48].

While this work focuses on the inverse design of modular metamaterials targeting uniaxial stress–strain responses, it demonstrates the feasibility of employing DL to accelerate metamaterial discovery. Future studies can extend this framework to the inverse design of anisotropic mechanical responses in multiple directions and to broader design spaces encompassing modules with diverse mechanical behaviors. Incorporating active materials that respond to environmental stimuli such as temperature, light, or magnetic fields may further embed intelligence within the metamaterial itself, paving the way toward intelligent materials [17,49]. When combined with autonomous robotic assembly and reassembly, such reprogrammable and reconfigurable modular metamaterial systems promise versatility, robustness, and cost efficiency through scalability, reuse, and generality—unlocking new opportunities in aerospace structures, exploration, and adaptive engineering systems [43].

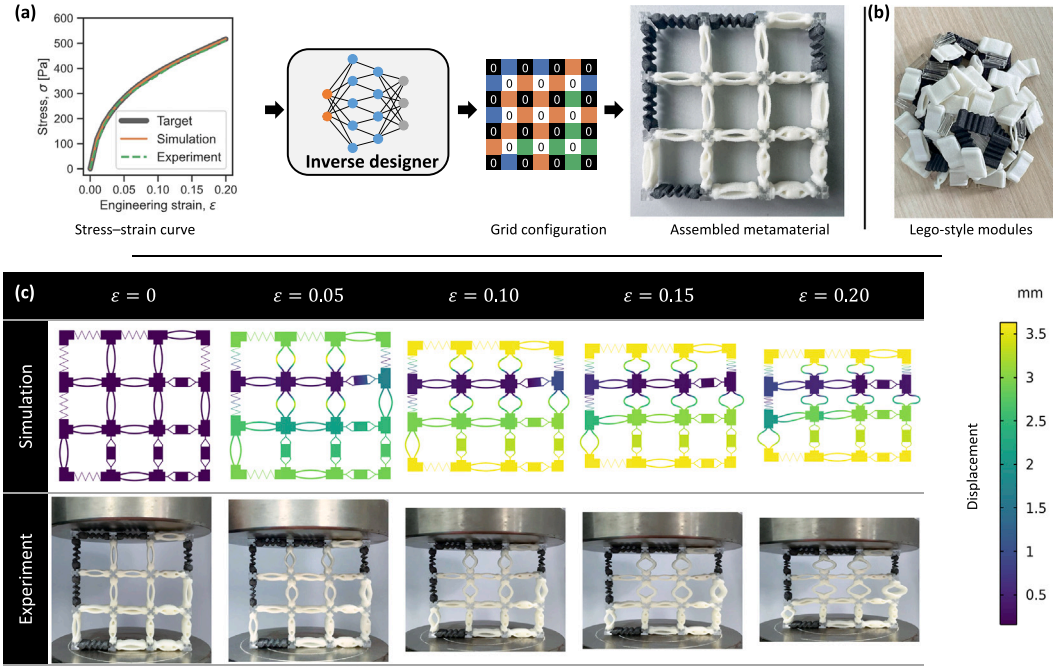

Fig. 7. Demonstration of the inverse designer for modular metamaterial design and fabrication. (a) Generation of a modular metamaterial using the 2D inverse designer given a target stress–strain curve, followed by prototype assembly. (b) Photographs of 3D-printed Lego-style modules used for experimental assembly. (c) Comparison of the nonlinear mechanical responses obtained from uniaxial compression testing and FEM simulation.

4. Experimental section

4.1. Dataset preparation

Two datasets were prepared for the DL training of 2D and 3D modular metamaterials, respectively. For the 2D dataset, we generated $N = 60,000$ modular metamaterials with random 7×7 grid configurations composed of three basic ligament modules. The corresponding stress–strain curves were obtained through FEM simulations using COMSOL Multiphysics (version 6.2, COMSOL, Sweden). The simulations followed a representative volume element (RVE) approach [50,51], in which a perturbation displacement field was solved under prescribed macroscopic strain or stress modes. In the simulations, a hard rubber-like material (incompressible neo-Hookean hyperelastic model, $E = 85$ MPa) was used for the linear module, a soft rubber-like material (incompressible neo-Hookean hyperelastic model, $E = 3.35$ MPa) was used for the yielding-like and snap-through buckling modules, and a rigid resin (elastic model, $E = 1.6$ GPa, $\nu = 0.23$) was used for the node joints, all of which correspond to 3D-printable materials. Because of the low density of the hollow microstructures, self-weight effects were neglected. A macroscopic uniaxial compressive stress was applied to each RVE until a strain of $\varepsilon = 0.2$ in the vertical direction was reached, yielding the macroscopic stress–strain curves. In the labeled 2D dataset, each data point consists of a grid representation x (a 7×7 matrix composed of integers 0, 1, 2, and 3 corresponding to node and ligament modules) and its corresponding stress–strain curve y, denoted as $S = \{\mathbf{x}, \mathbf{y}\}_{i=1}^{N}$. Fig. S3 shows the distribution of stress–strain curves in the 2D dataset. Similarly, a 3D dataset was prepared using the same procedure, where the grid representation x has a shape of $5 \times 5 \times 5$. Fig. S4 visualizes the distribution of stress–strain curves for the 3D dataset.

4.2. Deep learning implementation

All deep learning models were implemented in TensorFlow (version 2.12.0) and trained on a single NVIDIA RTX A6000 graphics card (48 GB GPU memory) running on a Linux system. The software environment was configured with Python 3.10 and CUDA 11.8. Model training was performed using the Adam optimizer with a learning rate of 1×10^{-4}, and the dataset was split into training and validation sets with a 0.8/0.2 ratio. Details of the model architectures and training procedures are provided in the Supporting Information. The complete codebase, including model definitions and training scripts, is publicly available at: https://github.com/xyzheng-ut/Legometa.

4.3. Mechanical testing

Prototypes of the modular metamaterials were fabricated by assembling 3D-printed modules. To suppress out-of-plane buckling, the prototypes were 3D-printed with a thickness of 10 mm, which is sufficient to prevent global out-of-plane instability during compression testing. The node joints, linear modules, and yielding-like and snap-through buckling modules were fabricated using a clear resin (Clear Resin V4, Formlabs, USA), flexible thermoplastic polyurethane (TPU) powder (Ultrasint TPU01, BASF SE, Germany), and elastic TPU powder (Elastollan, BASF SE, Germany), respectively—corresponding to the material models used in the FEM simulations. The modular metamaterials were manually assembled from these printed components. Uniaxial compression tests were conducted using a motorized test stand (ETM104C-10kN, Shenzhen Wance Testing Equipment Co., Ltd., China) to evaluate the mechanical properties of the assembled structures. The deformation rate was set to 0.5 mm/min, with the test terminated at a compressive strain of 0.2. The deformation processes were recorded using a high-speed camera capturing the front view, and stress–strain curves were obtained from the measured load and displacement data.

CRediT authorship contribution statement

Xiaofeng Guo: Writing – review & editing, Writing – original draft, Visualization, Validation, Software, Investigation, Formal analysis, Data curation. **Miaomiao He:** Writing – review & editing, Investigation, Formal analysis, Data curation. **Ikumu Watanabe:** Writing – review & editing, Investigation, Conceptualization. **Jiaxin Zhou:** Writing – review & editing, Investigation. **Takayuki Yamada:** Writing – review

& editing, Software, Resources. **Yong Yi:** Writing – review & editing, Supervision, Resources, Project administration, Funding acquisition. **Xiaoyang Zheng:** Writing – review & editing, Writing – original draft, Visualization, Supervision, Software, Project administration, Methodology, Funding acquisition, Conceptualization.

Declaration of competing interest

The authors declare that they have no known competing financial interests or personal relationships that could have appeared to influence the work reported in this paper.

Acknowledgments

X.G. acknowledges their NIMS Internship Program for the stay and research in Japan. X.Z. acknowledges the financial support from the Google Research Grant and the Hirose Foundation Grant.

Appendix A. Supplementary data

Supplementary data for this article can be found online at doi:10.1016/j.matdes.2026.115584.

Data availability

Data will be made available on request.

References

[1] X. Zheng, X. Zhang, T.-T. Chen, I. Watanabe, Deep learning in mechanical metamaterials: from prediction and generation to inverse design, Adv. Mater. 35 (45) (2023) 2302530.
[2] X. Xia, C.M. Spadaccini, J.R. Greer, Responsive materials architected in space and time, Nat. Rev. Mater. 7 (9) (2022) 683–701.
[3] P. Jiao, J. Mueller, J.R. Raney, X. Zheng, A.H. Alavi, Mechanical metamaterials and beyond, Nature Commun. 14 (1) (2023) 6004.
[4] P. Sinha, T. Mukhopadhyay, Programmable multi-physical mechanics of mechanical metamaterials, Mater. Sci. Eng. R Rep. 155 (2023) 100745.
[5] K.K. Dudek, M. Kadic, C. Coulais, K. Bertoldi, Shape-morphing metamaterials, Nat. Rev. Mater. 10 (10) (2025) 783–798.
[6] T.A. Schaedler, A.J. Jacobsen, A. Torrents, A.E. Sorensen, J. Lian, J.R. Greer, L. Valdevit, W.B. Carter, Ultralight metallic microlattices, Science 334 (6058) (2011) 962–965.
[7] D. Rayneau-Kirkhope, Y. Mao, R. Farr, Ultralight fractal structures from hollow tubes, Phys. Rev. Lett. 109 (20) (2012) 204301.
[8] X. Zheng, X. Guo, I. Watanabe, A mathematically defined 3D auxetic metamaterial with tunable mechanical and conduction properties, Mater. Des. 198 (2021) 109313.
[9] J. Zhou, I. Watanabe, K. Kambayashi, Computational design of mechanical metamaterials through misaligned periodic microstructure, Mater. Des. 253 (2025) 113819.
[10] D. Akamatsu, Y. Noguchi, K. Matsushima, Y. Sato, J. Yanagimoto, T. Yamada, Two-phase topology optimization for metamaterials with negative poisson's ratio, Composite Struct. 311 (2023) 116800.
[11] L. Jin, R. Khajehtourian, J. Mueller, A. Rafsanjani, V. Tournat, K. Bertoldi, D.M. Kochmann, Guided transition waves in multistable mechanical metamaterials, Proc. Natl. Acad. Sci. 117 (5) (2020) 2319–2325.
[12] H. Xiu, H. Liu, A. Poli, G. Wan, K. Sun, E.M. Arruda, X. Mao, Z. Chen, Topological transformability and reprogrammability of multistable mechanical metamaterials, Proc. Natl. Acad. Sci. 119 (52) (2022) e2211725119.
[13] Y. Hong, C. Zhou, H. Qing, Y. Chi, J. Yin, Reprogrammable snapping morphogenesis in ribbon-cluster meta-units using stored elastic energy, Nat. Mater. 24 (2025) 1793–1801.
[14] J.L. Silverberg, A.A. Evans, L. McLeod, R.C. Hayward, T. Hull, C.D. Santangelo, I. Cohen, Using origami design principles to fold reprogrammable mechanical metamaterials, Science 345 (6197) (2014) 647–650.
[15] J. Qi, Z. Chen, P. Jiang, W. Hu, Y. Wang, Z. Zhao, X. Cao, S. Zhang, R. Tao, Y. Li, et al., Recent progress in active mechanical metamaterials and construction principles, Adv. Sci. 9 (1) (2022) 2102662.
[16] X. Zheng, K. Uto, W.-H. Hu, T.-T. Chen, M. Naito, I. Watanabe, Reprogrammable flexible mechanical metamaterials, Appl. Mater. Today 29 (2022) 101662.
[17] X. Zheng, Y. Jiang, M. Mete, J. Li, I. Watanabe, T. Yamada, J. Paik, Metamaterial Robotics, Sci. Robot. 10 (108) (2025) eadx1519, https://doi.org/10.1126/scirobotics.adx1519
[18] Q. Guan, B. Dai, H.H. Cheng, J. Hughes, Lattice structure musculoskeletal robots: harnessing programmable geometric topology and anisotropy, Sci. Adv. 11 (29) (2025) eadu9856.
[19] U. Tanriverdi, G. Senesi, T. Asfour, H. Kurt, S.L. Smith, D. Toderita, J. Shalhoub, L. Burgess, A.M. Bull, F. Güder, Dynamically adaptive soft metamaterial for wearable human–machine interfaces, Nature Commun. 16 (1) (2025) 2621.
[20] H. Cheng, X. Zhu, X. Cheng, P. Cai, J. Liu, H. Yao, L. Zhang, J. Duan, Mechanical metamaterials made of freestanding quasi-BCC nanolattices of gold and copper with ultra-high energy absorption capacity, Nat. Commun. 14 (1) (2023) 1243.
[21] M. Carton, J.F. Kowalewski, J. Guo, J.F. Alpert, A. Garg, D. Revier, J.I. Lipton, Bridging hard and soft: mechanical metamaterials enable rigid torque transmission in soft robots, Sci. Robot. 10 (100) (2025) eads0548.
[22] M. Kalogeropoulou, A. Kracher, P. Fucile, S.M. Mihăilă, L. Moroni, Blueprints of architected materials: a guide to metamaterial design for tissue engineering, Adv. Mater. 36 (47) (2024) 2408082.
[23] Y. Qin, Z. Jing, D. Zou, Y. Wang, H. Yang, K. Chen, W. Li, P. Wen, Y. Zheng, A metamaterial scaffold beyond modulus limits: enhanced osteogenesis and angiogenesis of critical bone defects, Nat. Commun. 16 (1) (2025) 2180.
[24] H. Yasuda, P.R. Buskohl, A. Gillman, T.D. Murphey, S. Stepney, R.A. Vaia, J.R. Raney, Mechanical computing, Nature 598 (7879) (2021) 39–48.
[25] R.H. Lee, E.A. Mulder, J.B. Hopkins, Mechanical neural networks: architected materials that learn behaviors, Sci. Robot. 7 (71) (2022) eabq7278.
[26] X. Zhang, Y. Wang, Z. Tian, M. Samri, K. Moh, R.M. McMeeking, R. Hensel, E. Arzt, A bioinspired snap-through metastructure for manipulating micro-objects, Sci. Adv. 8 (46) (2022) eadd4768.
[27] P. Ducarme, B. Weber, M. van Hecke, J.T. Overvelde, Exotic mechanical properties enabled by countersnapping instabilities, Proc. Natl. Acad. Sci. 122 (16) (2025) e2423301122.
[28] M. Zaiser, S. Zapperi, Disordered mechanical metamaterials, Nat. Rev. Phys. 5 (11) (2023) 679–688.
[29] M. Kadic, G.W. Milton, M. van Hecke, M. Wegener, 3D metamaterials, Nat. Rev. Phys. 1 (3) (2019) 198–210.
[30] S. Bonfanti, S. Hiemer, R. Zulkarnain, R. Guerra, M. Zaiser, S. Zapperi, Computational design of mechanical metamaterials, Nat. Comput. Sci. 4 (8) (2024) 574–583.
[31] D. Lee, W. Chen, L. Wang, Y.-C. Chan, W. Chen, Data-driven design for metamaterials and multiscale systems: a review, Adv. Mater. 36 (8) (2024) 2305254.
[32] X. Guo, X. Zheng, J. Zhou, T. Yamada, Y. Yi, I. Watanabe, Spring-based mechanical metamaterials with deep-learning-accelerated design, Mater. Des. 252 (2025) 113800.
[33] S. Kumar, S. Tan, L. Zheng, D.M. Kochmann, Inverse-designed spinodoid metamaterials, NPJ Comput. Mater. 6 (1) (2020) 73.
[34] J.K. Wilt, C. Yang, G.X. Gu, Accelerating auxetic metamaterial design with deep learning, Adv. Eng. Mater. 22 (5) (2020) 1901266.
[35] X. Zheng, T.-T. Chen, X. Guo, S. Samitsu, I. Watanabe, Controllable inverse design of auxetic metamaterials using deep learning, Mater. Des. 211 (2021) 110178.
[36] X. Zheng, T.-T. Chen, X. Jiang, M. Naito, I. Watanabe, Deep-learning-based inverse design of three-dimensional architected cellular materials with the target porosity and stiffness using voxelized voronoi lattices, Sci. Technol. Adv. Mater. 24 (1) (2023) 2157682.
[37] L. Wang, Y.-C. Chan, F. Ahmed, Z. Liu, P. Zhu, W. Chen, Deep generative modeling for mechanistic-based learning and design of metamaterial systems, Comput. Methods Appl. Mech. Eng. 372 (2020) 113377.
[38] J.-H. Bastek, D.M. Kochmann, Inverse design of nonlinear mechanical metamaterials via video denoising diffusion models, Nat. Mach. Intell. 5 (12) (2023) 1466–1475.
[39] X. Zheng, J. Shiomi, T. Yamada, Optimizing metamaterial inverse design with 3D conditional diffusion model and data augmentation, Adv. Mater. Technol. 10 (14) (2025) 2500293.
[40] M. Maurizi, D. Xu, Y.-T. Wang, D. Yao, D. Hahn, M. Oudich, A. Satpati, M. Bauchy, W. Wang, Y. Sun, et al., Designing metamaterials with programmable nonlinear responses and geometric constraints in graph space, Nat. Mach. Intell. 7 (2025) 1023–1036.
[41] K. Yang, L. Rao, L. Hu, F. Pan, Q. Yin, Y. Chen, Flexible, efficient and adaptive modular impact-resistant metamaterials, Int. J. Mech. Sci. 239 (2023) 107893.
[42] Z. Li, Y. Zhu, K. Yang, Modular metamaterials with strong auxeticity, tunability and crashworthiness, Int. J. Solids Struct. (2025) 113577.
[43] C.E. Gregg, D. Catanoso, O.I.B. Formoso, I. Kostitsyna, M.E. Ochalek, T.J. Olatunde, I.W. Park, F.M. Sebastianelli, E.M. Taylor, G.T. Trinh, et al., Ultralight, strong, and self-reprogrammable mechanical metamaterials, Sci. Robot. 9 (86) (2024) eadi2746.
[44] B. Saintyves, M. Spenko, H.M. Jaeger, A self-organizing robotic aggregate using solid and liquid-like collective states, Sci. Robot. 9 (86) (2024) eadh4130.
[45] T. Zhao, X. Dang, K. Manos, S. Zang, J. Mandal, M. Chen, G.H. Paulino, Modular chiral origami metamaterials, Nature 640 (8060) (2025) 931–940.
[46] J. Chen, Z. Wei, X. Xiao, K. Wei, X. Yang, Z. Qu, D. Fang, Mining extreme properties from a large metamaterial database, Nat. Commun. 16 (1) (2025) 9648.
[47] F. Stella, C.D. Santina, J. Hughes, How can LLMs transform the robotic design process? Nat. Mach. Intell. 5 (6) (2023) 561–564.
[48] G.E. Karniadakis, I.G. Kevrekidis, L. Lu, P. Perdikaris, S. Wang, L. Yang, Physics-informed machine learning, Nat. Rev. Phys. 3 (6) (2021) 422–440.
[49] D. Howard, A.E. Eiben, D.F. Kennedy, J.-B. Mouret, P. Valencia, D. Winkler, Evolving embodied intelligence from materials to machines, Nat. Mach. Intell. 1 (1) (2019) 12–19.
[50] I. Watanabe, A. Yamanaka, Voxel coarsening approach on image-based finite element modeling of representative volume element, Int. J. Mech. Sci. 150 (2019) 314–321.
[51] I. Watanabe, D. Setoyama, N. Nagasako, N. Iwata, K. Nakanishi, Multiscale prediction of mechanical behavior of ferrite–pearlite steel with numerical material testing, Int. J. Numer. Methods Eng. 89 (7) (2012) 829–845.